Variational Data Assimilation Experiments of Mei-Yu Front Rainstorms in China

WANG Yunfeng*[1,2] (王云峰), WANG Bin[1] (王 斌), HAN Yueqi[2] (韩月琪), ZHU Min[2] (朱 民)
HOU Zhiming[2] (侯志明), ZHOU Yi[2](周 毅), LIU Yudi[2] (刘宇迪), and KOU Zheng[2](寇 正)

[1] *State Key Laboratory of Numerical Modeling for Atmospheric Sciences and Geophysical Fluid Dynamics, Institute of Atmospheric Physics, Chinese Academy of Sciences, Beijing* 100029

[2] *Institute of Meteorology, PLA University of Science and Technology, Nanjing* 211101

(Received 4 March 2003; revised 5 December 2003)

ABSTRACT

The numerical forecasts of mei-yu front rainstorms in China has been an important issue. The intensity and pattern of the frontal rainfall are greatly influenced by the initial fields of the numerical model. The 4-dimensional variational data assimilation technology (4DVAR) can effectively assimilate all kinds of observed data, including rainfall data at the observed stations, so that the initial fields and the precipitation forecast can both be greatly improved. The non-hydrostatic meso-scale model (MM5) and its adjoint model are used to study the development of the mei-yu front rainstorm from 1200 UTC 25 June to 0600 UTC 26 June 1999. By numerical simulation experiments and assimilation experiments, the T106 data and the observed 6-hour rainfall data are assimilated. The influences of many factors, such as the choice of the assimilated variables and the weighting coefficient, on the precipitation forecast results are studied. The numerical results show that 4DVAR is valuable and important to mei-yu front rainfall prediction.

Key words: mei-yu front rainstorm, 4DVAR, MM5 model and its adjoint model

1. Introduction

The numerical forecast of mei-yu front rainstorms in China has been an important issue and difficult to deal with. A lot of important research work has already been done, not only studying dynamics theory, but also performing the numerical simulating experiments (Zhou et al., 1984; Chen et al., 1995; Zhu et al., 1998). Since the 1980s, many field experiments and rainstorm research plans were performed in China to study the meso-scale convective system of the mei-yu front, especially to study its mechanism of occurrence, development, and maintenance. Many basic concepts have been clarified, such as the importance of the large-scale background fields to the occurrence of the mei-yu front rainfall, the 3-dimensional structure and the evolution mechanism of the meso-scale rainstorm system, the interaction mechanism between different scale weather systems, and so on. But the distribution pattern and the intensity of the mei-yu front rainfall are still difficult to predict. The forecast of the mei-yu front rainfall is very difficult because of the interaction between weather systems with different spatial and temporal scales. Undoubtedly, the proper large-scale background fields are very important to the prediction of the mei-yu front rainfall. However the development of the mei-yu front rainstorm system is also based on the meso-scale structure of the initial fields, such as temperature, humidity, and wind. Sometimes, if the initial fields are obtained only based on traditional large-scale observed data, the forecasts for the first 6 hours or 12 hours will have large errors. Thus it is very important for a numerical forecast model to have accurate physical processes on the one hand, while to have accurate initial fields on the other hand, as much as possible.

4DVAR was introduced into meteorological fields of study in the 1980s (Lewis and Derber, 1985; Le Dimet and Talagrand, 1986; Talagrand and Courtier, 1987). Afterwards, it was widely used in atmospheric and oceanic research fields (Derber, 1987; Navon and Legler, 1987; Chao and Chang, 1992; Gao and Chou,

*E-mail: wangyf@mail.iap.ac.cn

1994; Zhu, 1995; Wang et al., 2000a, b; Zou et al., 1993, 1999, 2000; Wang and Wang, 2003). However, few people studied the mei-yu front rainstorm in China with 4DVAR. In this paper, the MM5 model and its adjoint model are used to study a mei-yu front rainstorm from 1200 UTC 25 June to 0600 UTC 26 June 1999. Numerical simulation experiments and assimilation experiments are designed to study the effects of different factors, such as the choice of the assimilating variables, the way to calculate the weighting coefficient, etc. The T106 data and the observed 6-hour rainfall data are used in these experiments. The variational assimilation principle for rainfall data is introduced in section 2, the numerical experiments are presented in section 3, and the conclusion is given in section 4.

2. The variational assimilation principle of rainfall data

Taking advantage of the observed data which vary with time, and regarding the forecast equations as the constrained conditions, we use 4DVAR to find the optimal initial conditions for the numerical forecast model and to minimize the cost function, which denotes the distance between the model forecasted and the observed data. In other words, 4DVAR can convert temporal information of observed data to spatial information of the initial conditions.

In this paper, the cost function J is defined as

$$J = J_{\rm M} + J_{\rm R} \ . \tag{1}$$

Here, $J_{\rm M}$ is the distance between the model control variables and the corresponding observed variables; $J_{\rm R}$ is the distance between the predicted mei-yu front rainfall and the observed rainfall. They are defined as

$$J_{\rm M}=\sum_{k=0}^{K}[\boldsymbol{X}(t_k)-\boldsymbol{X}_{\rm obs}(t_k)]^{\rm T}\boldsymbol{W}_X[\boldsymbol{X}(t_k)-\boldsymbol{X}_{\rm obs}(t_k)] \ , \tag{2}$$

and

$$J_{\rm R} = \sum_{m=1}^{M}[\boldsymbol{R}_m - \boldsymbol{R}_{m,{\rm obs}}]^{\rm T}\boldsymbol{W}_{\rm R}[\boldsymbol{R}_m - \boldsymbol{R}_{m,{\rm obs}}] \ . \tag{3}$$

Here, t is the observed time, $k = 1, 2, \ldots, K$ indexes the observed times of the model control variables, and $m = 1, 2, \ldots, M$ indexes the observed times of the station rainfall data. $\boldsymbol{X}$ is the model control variable. $\boldsymbol{R}$ is the rainfall. The subscript "obs" and superscript "T" denote the observed data and the transpose of the matrix, respectively. $\boldsymbol{W}_X$ is the weighting coefficient of the model control variable, and $\boldsymbol{W}_{\rm R}$ is the weighting coefficient of the rainfall. Both the model control variable $\boldsymbol{X}(t_k)$ and predicted rainfall $\boldsymbol{R}_m$ depend on the initial fields $\boldsymbol{X}(t_0)$, so that the cost function J can be defined as $J = J[\boldsymbol{X}(t_0)]$, and $\boldsymbol{R}$ can be defined as $\boldsymbol{R} = \boldsymbol{A}[\boldsymbol{X}(t_0)]$, where $\boldsymbol{A}$ is the observed operator. $\boldsymbol{A}$ can be regarded as a calculation procedure in the numerical model, which calculates the predicted rainfall by using the model control variables (temperature, pressure, wind, etc.). $\boldsymbol{A}$ includes the large-scale precipitation scheme, the cumulus convective parameterization scheme, and the calculation procedure of changing the rainfall values from grids to stations.

The initial fields can be optimized by the following equation:

$$\boldsymbol{X}_{n+1}(t_0) = \boldsymbol{X}_n(t_0) - (\rho\nabla J)_n \ , \tag{4}$$

where $n = 1, 2, \ldots, N$ is the iteration index, ρ is the optimal step size, and $\nabla J = \nabla J_{\rm M} + \nabla J_{\rm R}$ is the gradient. In order to minimize the cost function J and obtain the optimal initial fields $\boldsymbol{X}(t_0)$, the gradient ∇J must be calculated first by using the adjoint model. The way to calculate $\nabla J_{\rm M}$ can be found in some references (Lewis and Derber, 1985; Le Dimet and Talagrand, 1986; and Navon et al., 1992). In this paper, the procedure for calculating $\nabla J_{\rm R}$ is introduced.

The first-order perturbation $\boldsymbol{X}'(t_0)$ of the initial fields $\boldsymbol{X}(t_0)$ can bring the first-order perturbation $\boldsymbol{R}'_m$ of the rainfall $\boldsymbol{R}_m$, where $\boldsymbol{R}'_m = \boldsymbol{Q}_m[\boldsymbol{X}'(t_0)]$, and $\boldsymbol{Q}_m$ is the tangent linear operator of $\boldsymbol{A}$, which can be used to calculate $\boldsymbol{R}'_m$ from $\boldsymbol{X}'(t_0)$.

The first-order perturbation $J'_{\rm R}$ of the cost function $J_{\rm R}$ can be obtained from equation (5) as follows:

$$J'_{\rm R}[\boldsymbol{X}(t_0)] = \sum_{m=1}^{M} 2\boldsymbol{W}_{\rm R}[\boldsymbol{R}_m - \boldsymbol{R}_{m,{\rm obs}}]^{\rm T}\boldsymbol{R}'_m \ . \tag{5}$$

Replacing $\boldsymbol{R}'_m$ by $\boldsymbol{Q}_m[\boldsymbol{X}'(t_0)]$ into equation (3), we have

$$J'_{\rm R}[\boldsymbol{X}(t_0)] = \sum_{m=1}^{M} 2\boldsymbol{W}_{\rm R}[\boldsymbol{R}_m - \boldsymbol{R}_{m,{\rm obs}}]^{\rm T}\boldsymbol{Q}_m[\boldsymbol{X}'(t_0)] \ . \tag{6}$$

Moreover, there exists

$$J'_{\rm R}[\boldsymbol{X}(t_0)] = \{\nabla J_{\rm R}[\boldsymbol{X}(t_0)]\}^{\rm T}\boldsymbol{X}'(t_0) \ . \tag{7}$$

From equations (6) and (7), there is

$$\nabla J_{\rm R}[\boldsymbol{X}(t_0)] = \sum_{m=1}^{M} \boldsymbol{Q}^*_m 2\boldsymbol{W}_{\rm R}[\boldsymbol{R}_m - \boldsymbol{R}_{m,{\rm obs}}] \ , \tag{8}$$

where $\boldsymbol{Q}^*_m$ is the adjoint operator of $\boldsymbol{Q}_m$. The method of obtaining $\boldsymbol{Q}_m$ and $\boldsymbol{Q}^*_m$ from the observed operator $\boldsymbol{A}$ can be found in Zou et al. (1993, 1999).

Because the adjoint model is linear, $\nabla J_{\rm R}$ can be obtained by integrating the adjoint model only once from the final time t_K backward to t_0 and continuously adding the forcing term $2\boldsymbol{W}_{\rm R}[\boldsymbol{R}_m - \boldsymbol{R}_{m,{\rm obs}}]$ to

the adjoint variables at the observed time t_m, giving the final result of ∇J_{R}.

The above principle of variational assimilation about assimilating the observed rainfall can also be used to assimilate the non-conventional observed data, such as satellite data and radar data, while the observed operator $\boldsymbol{A}$ denotes the calculating procedure from model control variables to satellite data or radar data.

3. Numerical experiments

In this paper, the MM5 model and its adjoint model are used to study the mei-yu front rainstorm from 1200 UTC 25 June to 0600 UTC 26 June 1999. The center point of the calculation region is (32.0°N, 118.0°E). The number of horizontal grid points is 61×61, and the grid interval is 45 kilometers. The number of vertical levels is 11. The T106 data and the observed rainfall data, with time intervals of 12 hours and 6 hours respectively, are used in the numerical experiments.

Some numerical simulation experiments and assimilation experiments are designed to study the effect of different factors on the forecasted precipitation, such as the setting of the integration time step size, the choice of assimilation variables, and how to calculate the weighting coefficient. The details follow.

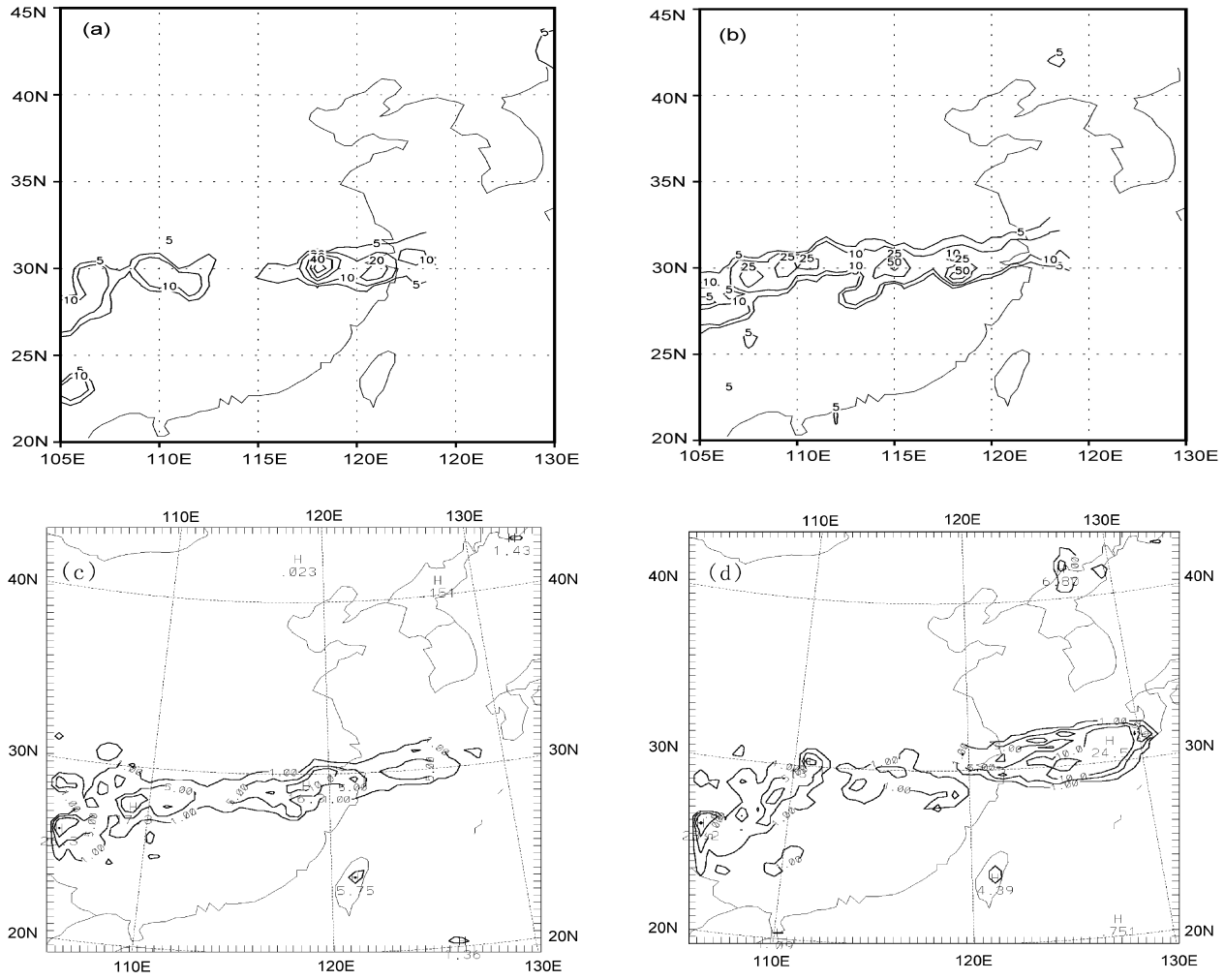

Fig. 1. The 6-hour rainfall distribution patterns of the observed data and the control experiment Expt. 0 (units: mm). (a) the first 6-hour rainfall pattern (observational data), (b) the second 6-hour rainfall pattern (observational data), (c) the first 6-hour rainfall pattern (control experiment), (d) the second 6-hour rainfall pattern (control experiment).

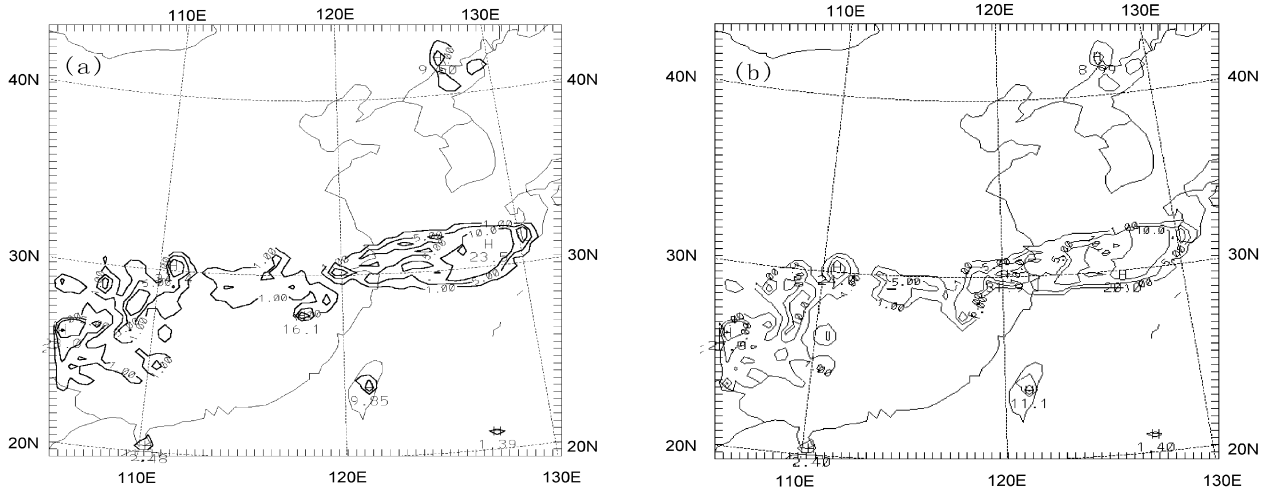

Fig. 2. The distribution patterns of the second 6-hour rainfall (unitm: mm). (a) Sensitivity experiment Expt. 1; the forecast time step size is 60 second. (b) Assimilation experiment Expt. 2; the frist 6-hour rainfall is assimilated.

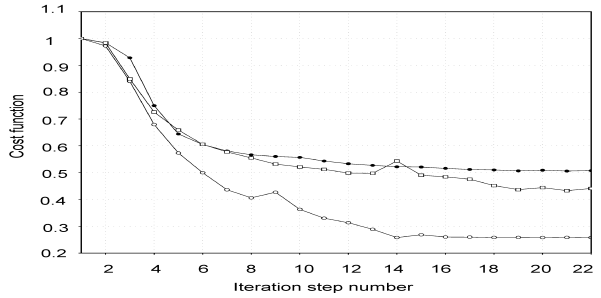

Fig. 3. The variation of the standardized cost function with iteration step number in different variational assimilation experiments: Expt. 3, hollow dot; Expt. 4, solid dot; Expt. 5 hollow square.

3.1 *Control experiment, sensitivity experiment, and variational assimilation experiment*

In the control experiment Expt. 0, the initial time is 1200 UTC 25 June. The initial fields and the boundary conditions are made from T106 data, without assimilating any data. The step size is 120 seconds. The forecast model is integrated for 18 hours, and the rainfall prediction is given out every 6 hours.

The 6-hour rainfall distribution patterns of the observed data and those in the control experiment Expt. 0 for 1200–1800 UTC 25 June are shown in Figs. 1a and 1c, respectively. The observed rainfall pattern exhibits an east-west oriented narrow band about the latitude line of 30°N with a few centers (Fig. 1a). A similar narrow band rainfall pattern is also found in Expt. 0 (Fig. 1c). However, not all the positions and intensities of the centers within the rainband are close to those of the observed data. In some cases of Expt.0, the position of the center is close to the observed one, but its intensity is much less than the observed one. For example, a rainfall center in Expt. 0 in Fig. 1c is located near (30°N, 118°E), which is close to that of the observed data in Fig. 1a. But the precipitation intensity in Fig. 1a is 16.3 mm, while in Fig. 1c it is 44 mm. However the precipitation intensity in Fig. 1a is almost same as the observed data. In some other cases, the intensity of a center in Expt. 0 is close to the observed one, but its position may be far apart from the observed one. For example, a rainfall center of Expt. 0, which is located near (27°N, 109°E), is to the south of the observed data by about 2–3 degrees. The second 6-hour rainfall distribution pattern of the observed data and that in the control experiment Expt. 0 from 1800 UTC 25 June to 0000 UTC 26 June are shown in Figs. 1b and 1d, respectively. The precipitation intensities of the observed data, with two centers located at (30°N, 115°E) and (30°N, 118°E) respectively, both exceed 50 mm, while in Expt. 0 they are only several mm. Both the above rainfall centers in Expt. 0 are located to the east of the corresponding observed rainfall centers. And the rainfall center of Expt. 0, which is located near 110°E, is still located to the south of the observed data.

The comparison, shown in Fig. 1, indicates that the MM5 model has the ability to simulate the mei-yu front rainstorm to some degree. If the initial fields are made only based on the T106 data, even though proper large-scale background fields are provided, the numerical simulation results would still not be satisfactory. For example, the forecasted center is located to the south of the observed center, and the forecasted

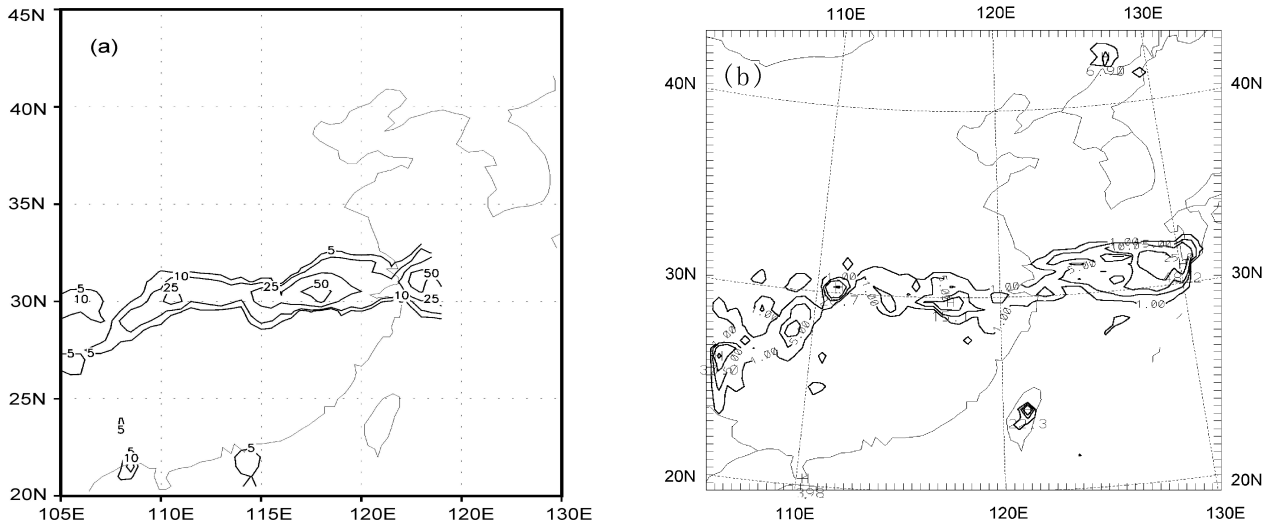

Fig. 4. The distribution patterns of the third 6-hour rainfall (units: mm). (a) observed data; (b) control experiment.

precipitation intensity is weaker than the observed one.

In the sensitivity experiment Expt. 1, the time step size is set as 60 seconds and the forecasted results are presented in Fig. 2a. It shows that the rainfall distribution pattern in Expt. 1 is also similar to that of the observed data. The rainfall center located near (30°N, 118°E), has been predicted and its precipitation intensity increases to 16.1 mm. Both its distribution pattern and intensity are better than those of the control experiment. But its intensity is still far smaller than that of the corresponding data. By comparing the sensitivity experiment with the control experiment, we find that properly decreasing the time step size may improve the accuracy of the forecasted rainfall. But the improvement is still not good enough for our purposes.

In the variational assimilation experiment Expt. 2, the first 6-hour observed rainfall data (from 1200 UTC 25 June to 1800 UTC 25 June) are assimilated to obtain the optimal initial fields. The forecasted distribution pattern of the second 6-hour rainfall is shown in Fig. 2b. Not only has the long, narrow rain belt been predicted properly, but both the center position and precipitation intensity of the rainfall are also improved. The precipitation intensity of a rainfall center, located near (30°N, 120°E) is increased to 31.9 mm. The corresponding value is about 5 mm in Expt. 0, while the observed value is about 50 mm. This shows that the variational assimilation experiment Expt. 2 is far better than the control experiment Expt. 0 and closer to the observed data. But the rainfall center in Expt. 2 is still located to the east of the observed one by about 1–2 degrees. For another rainfall center, near (30°N, 110°E), the intensity is also increased to 24.0 mm. Figure 2b also shows that the forecasted rainfall in Expt. 2 is larger than that in the control experiment Expt. 0 (13.1 mm) and almost as large as the observed rainfall (25 mm). From the above results, it is obvious that 4DVAR is very effective for rainfall forecasts in that it can improve both the distribution pattern and the intensity of the mei-yu rainfall.

During the iterative procedure, the cost function usually decreasies with each iterative step (figure not shown). Based on this fact, it is found that the method of assimilating the observed rainfall data is very effective to decrease the distance between the forecast rainfall and the observed rainfall. In fact, the cost function decreases very fast and almost reaches its minimum after only several iterative steps, and finally it can be decreased by about 65% of its initial value.

3.2 *Choosing different assimilated variables*

In order to compare the effect of assimilating different variables, three assimilation experiments are designed as in Table 1. In Expt. 3, two 6-hour observed rainfall records (from 1200 UTC 25 June to 1800 UTC 25 June and from 1800 UTC 25 June to 0000 UTC 26 June) are assimilated. In case 4, the T106 data at 0000 UTC 26 June are assimilated, including wind fields u and v, humidity fields q, and temperature fields t. Finally, the numerical forecast model is integrated for 18 hours with the optimal initial fields, and the forecast results are outputted every 6 hours.

Figure 3 is the variation of the cost function with the iterative number in different assimilation experiments.

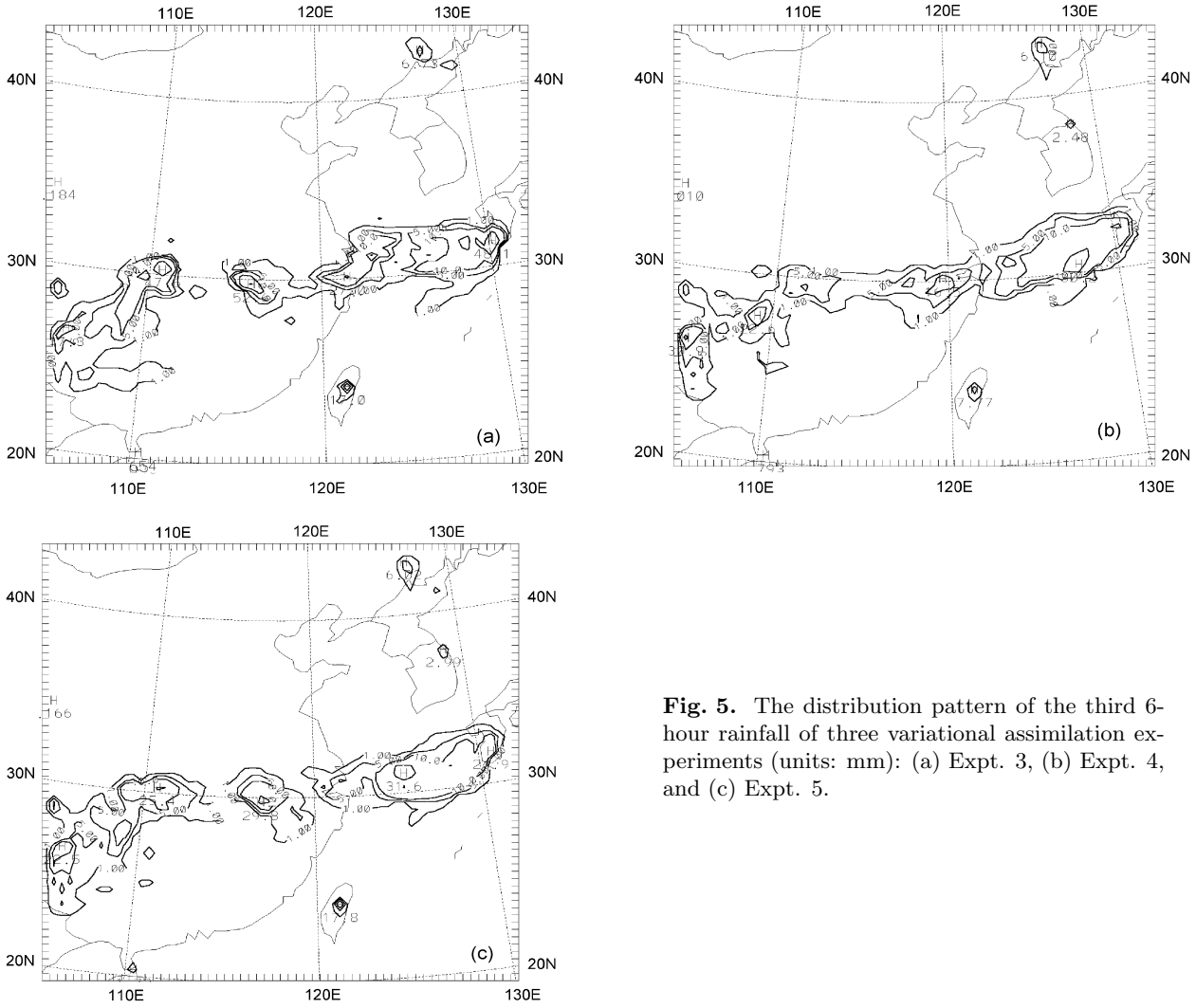

Fig. 5. The distribution pattern of the third 6-hour rainfall of three variational assimilation experiments (units: mm): (a) Expt. 3, (b) Expt. 4, and (c) Expt. 5.

Table 1. The experiments of assimilating different variables.

Experiments	Assimilated variables
Expt. 3	Two 6-hour rainfalls
Expt. 4	The T106 data (u, v, q, t) at 0000 UTC 26 June
Expt. 5	Two 6-hour rainfalls and the T106 data (u, v, q, t) at 0000 UTC 26 June

Among the three assimilation experiments, the cost functions all decrease by over 45%. The cost function decreases the most in Expt. 3 (74%), the least in Expt. 4 (49%), and moderately in Expt. 5 (56%). From the varation of the cost function, it can be found that the assimilation of the observed rainfall data and the T106 data is very valuable to the rainfall forecast. And, the changing value of the cost function is the largest only if assimilating the observed rainfall data.

The third 6-hour rainfall (from 0000 UTC 26 June to 0600 UTC 26 June) of the observed data and that of the control experiment are shown in Fig. 4. In the control experiment, the rainfall distribution pattern is very similar to that of the observed data. A rainfall center is located near (30°N, 110°E). Both its intensity and position are almost the same as those of the observed data. Another rainfall center is located near (31°N, 117°E). Its intensity (15.1 mm) is far smaller than that of the observed data (50 mm), and its position is to the south of the observed rainfall center by about 1 degree.

Figure 5 shows the distribution patterns of the third 6-hour rainfall for the three variational assimilation experiments, Expt. 3, Expt. 4, and Expt. 5.

From Fig. 5, it is found that the rainfall forecast can be improved as long as the observed data are assimilated. The rainfall distribution pattern and the rainfall intensity are closer to those of the observed

Table 2. The effect of the weighting coefficient of rainfall (the standard weighting coefficient is $W_0 = 20$).

Cost function	Experiment			
	1	2	3	4
$W_{\rm R}$	15	25	35	50
The cost function $J_{\rm M,0}$ of the model control variables	0.10804×10^5	0.10804×10^5	0.10804×10^5	0.10804×10^5
The cost function $J_{\rm R,\,0}$ of the rainfall	0.29513×10^4	0.49189×10^4	0.68865×10^4	0.98378×10^5
The total cost function $J_{\rm M,\,0} + J_{\rm R,\,0}$	0.13755×10^5	0.15723×10^5	0.17691×10^5	0.20642×10^5
The cost function $J_{\rm M,\,N}$ of the model control variables	0.54513×10^4	0.57881×10^4	0.60882×10^4	0.65988×10^4
The cost function $J_{\rm R,\,N}$ of the rainfall	0.10261×10^4	0.16129×10^4	0.15616×10^4	0.22319×10^4
The total cost function $J_{\rm M,\,N} + J_{\rm R,\,N}$	0.64774×10^4	0.74010×10^4	0.76498×10^4	0.88317×10^4
The cost function $I_{\rm R,\,N}$ of the standardizing weighting coefficient	0.13681×10^4	0.12903×10^4	0.08923×10^4	0.08928×10^4
The total cost function $J_{\rm M,\,N} + I_{\rm R,\,N}$ of the standardizing weighting coefficient	0.68194×10^4	0.70784×10^4	0.69805×10^4	0.74916×10^4

rainfall data than those of the control experiment. When the assimilated variables are different, the final effects on the simulated results are also different. In Fig. 5a, a rainfall center is located near (30°N, 116°E), which is to the west of the corresponding observed rainfall center. Its intensity is 52.6 mm, which is basically the same as the corresponding observed value (50 mm). Another rainfall center is near (30°N, 111°E), which is very close to the observed rainfall center. Its intensity is 47.6 mm, which is far larger than the observed rainfall intensity. In Fig. 5b, the transmeridional narrow distribution pattern of the rainfall is similar to the observed data, but the intensity of the rainfall is obviously weaker than that of the observed data. The intensity of the rainfall center located at (30°N, 119°E) is 16.5 mm, which is far smaller than that of the observed data. It is the same for the rainfall center located at (30°N, 111°E). In Fig. 5c, the rainfall distribution pattern is also similar to that of the observed data. The intensity of the rainfall center located at (30°N, 111°E) is 25.4 mm, which is almost the same as that of the observed data. The intensity of another rainfall center located at (30°N, 118°E) is 29.8 mm, which is weaker than the observed rainfall intensity, but far better than the control experiment. By comparison, case 5 is the best among the three assimilation experiments.

3.3 *The effect of the rainfall weighting coefficient*

Navon et al. (1992) pointed out that the weighting coefficient had two effects: (1) scaling the cost function and making it a non-dimensional variable; (2) denoting the quality reliability of the observed data. During the variational assimilation procedure, two types of data are provided: T106 data and the observed station rainfall data. The assimilated data include the model variables (u, v, q, t) and two 6-hour observed station rainfall datasets. A good weighting coefficient can correctly define the effect of different terms in the cost function and make the cost function decrease very fast. Thus how to choose the proper weighting coefficient of the rainfall is a very important problem. In Table 2, four experiments are designed with different weighting coefficients of rainfall. By comparing the variation of the cost function, the effect of the weighting coefficient is examined.

In these experiments, the weighting coefficients of rainfall are given as 15, 25, 35, and 50, respectively. Furthermore, the weighting coefficients of the model variables are given as

$$W_\psi(i,j,k) = \frac{1}{|\psi_{i,j,k,\rm obs}(t_0) - \psi_{i,j,k,\rm obs}(t_K)|^2} \ ,$$

where ψ is the model variable, (i, j, k) is the model grid index set, subscript "obs" denotes the observed data, and $t_0 \sim t_K$ is the assimilating window. In order to conveniently compare the effect of the cost function, a standardizing weighting coefficient W_0 of rainfall is introduced. The standardized equation is

$$I_{{\rm R},N} = J_{{\rm R},N} \times \boldsymbol{W}_0/\boldsymbol{W}_{\rm R} \ ,$$

where $J_{{\rm R},N}$ is the cost function of rainfall before standardization, $I_{{\rm R},N}$ is the cost function of the rainfall after standardization, subscript "N" is the final assimilation iterative step, and $\boldsymbol{W}_{\rm R}$ is the weighting coefficient of the rainfall. The total standardized cost function is $J_{{\rm M},N} + I_{{\rm R},N}$, where $J_{{\rm M},N}$ is the cost function of the model variables. It can be found from Table 2 that after standardization, the cost function of the third experiment is the smallest, and the smallest total

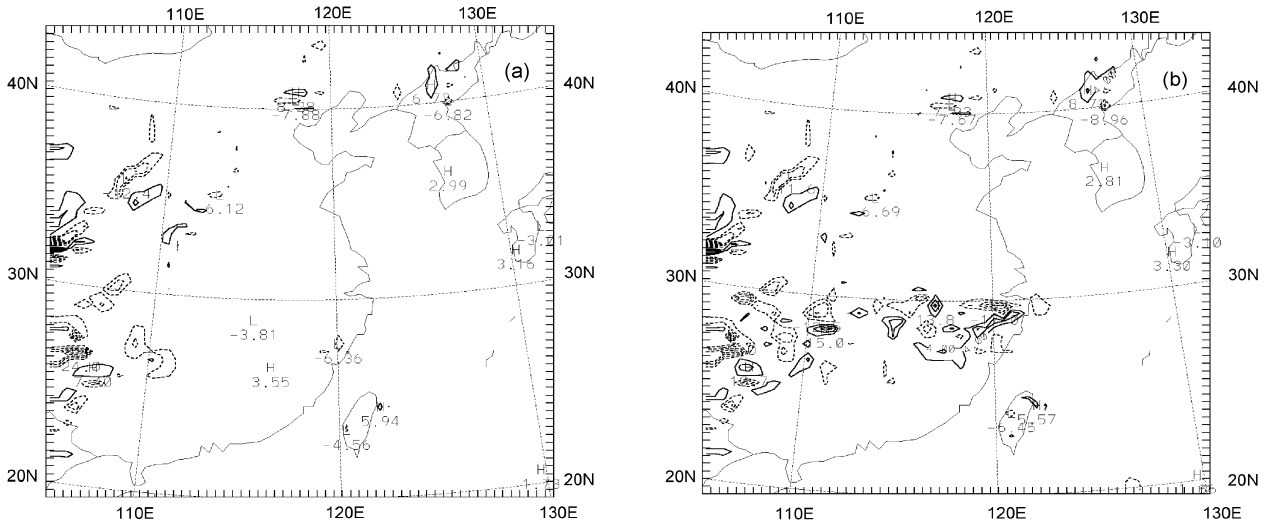

Fig. 6. The distribution pattern of the initial water vapor divergence fields at the 900-hPa isobaric surface (units: $1.0\times10^{-6}\,s^{-1}$: (a) before assimilation, and (b) after assimilation.

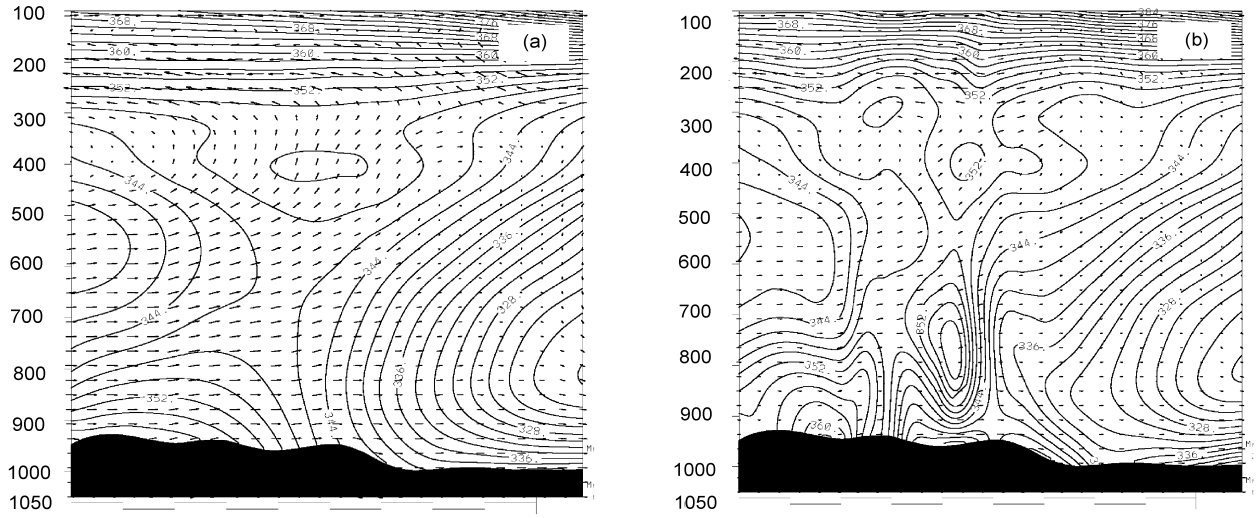

Fig. 7. The vertical section of the humidity potential temperature field (units: K): (a) before assimilation, and (b) after assimilation.

cost function is in the first experiment. Certainly in the assimilation experiments, the smaller the cost function is, the better the results are. In this paper, one of the research objectives is to study the effect of the choice of assimilation variables on the decrease of the cost function, because the cost function is relative to both the model variables and the observed rainfall data. Thus the principle of properly giving a weighting coefficient is to find which method can make the standardized total cost function very small and the standardized cost function of rainfall the smallest. Based on the above principle, the final weighting coefficient of the rainfall is given as 35.

3.4 *Improving the initial fields by variational assimilation*

During the objective analysis procedure of the numerical weather forecast, it is very easy to overly smooth the physical fields and lose much of the important meso-scale information, which may cause an inconsistency between the vapor fields and other physical fields, and then make the forecast results worse. The essence of 4DVAR is to optimize the initial fields– and therefore to improve the forecast results by taking

advantage of the valuable information of the observed data.

The distribution patterns of the initial water vapor divergence fields at the 900-hPa isobaric surface before and after assimilation are shown in Figs. 6a and 6b, respectively. From Fig. 6, we can find that before assimilation there are hardly any divergence centers in the initial fields. This is because the wind fields and the vapor fields have been overly smoothed during the objective analysis procedure. Thus there will be large deflection in the rainfall forecast results if the initial fields are made with T106 analysis data. We can also find that after assimilation many smaller-scale divergence centers appear in the optimal initial fields, whose distribution pattern is similar to that of the observed rainfall. This denotes that much of the important meso-scale information of the vapor fields has been retrieved from the optimal initial fields, so the initial water vapor fields can be properly described. Therefore, the resulting rainfall forecast can be effectively improved.

Figure 7 is the vertical section of the potential pseudo-equivalent temperature fields crossing the mei-yu front, whose center point is located at (30°N, 118°E). Figures 7a and 7b are the distribution patterns before and after assimilation, respectively. After assimilation, a meso-β-scale high-value center appears between 600 hPa and 900 hPa. The area of the potential instability region becomes large and the intensity increases. Because the potential instability region is related to the instability energy, and since the increasing of the instability energy is available to the formation and development of the rainfall system, the rainfall forecast will be improved after assimilation. The advantage of 4DVAR is that it converts the temporal information of the observed data into the spatial information of the initial fields and retrieves the meso-scale structure of the initial fields. Thus the initial fields and the rainfall forecast will be greatly improved.

4. Conclusions

In this paper, many numerical experiments and variational assimilation experiments of the mei-yu front rainstorm from 1200 UTC 25 June to 0600 UTC 26 June 1999 are designed. The influences of many factors on the forecasted rainfall precipitation are studied, such as the selection of the assimilation variables and the weighting coefficient. The following conclusions can be drawn:

(1) If the initial fields of the numerical model are given only by T106 data, it is not good enough for forecasting the mei-yu front rainfall forecast. Decreasing the time step size properly may improve the forecast of the rainfall, but the improvement is too small.

(2) When 4DVAR is introduced into the numerical experiments, no matter whether the model variable data or the observed rainfall data are assimilated, the forecasted results will be greatly improved.

(3) Assimilating the 6-hour rainfall data is able to improve the intensity forecasting. The forecasted rainfall is very close to the observed one, while the forecasted position of the rainfall center is displaced westward from the observed center. Assimilation of the model variables, such as u, v, q, t, w, and p', is very effective to improve the forecast of the rainfall pattern and the rainfall center position, but has little effect on the improvement of the rainfall intensity. For forecasting the intensity, only assimilating the observed data is more effective than assimilating the other model variables. It will be effective to both the rainfall distribution pattern and the rainfall intensity if both the model variables and the 6-hour observed rainfall data are assimilated simultaneously.

(4) The forecasted rainfall is also greatly influenced by the weighting coefficient. The proper weighting coefficient can make the cost function decrease very fast, and therefore improve the rainfall forecast.

Acknowledgments. This work was supported by the National Natural Science Foundation of China under Grant Nos. 40105012, 49928504, and 40221503, "973" Project under Grant No.G1999032801, and the Key Innovation Direction Project of the Chinese Academy of Sciences under Grant No. KZCX2208. The authors warmly thank Wu Rongsheng and Wang Yuan of Nanjing University for their valuable advice.

REFERENCES

Chao, W. C., and L. P. Chang, 1992: Development of a four-dimensional variational assimilation system using the adjoint method at GLA. Part I: Dynamics. *Mon. Wea. Rev.*, **120**, 1661–1673.

Chen Linsheng, Peng Xindong, and Ma Yan, 1995: Mesoscale numerical simulation of developing structure and evolution for vortex with heavy rain in Jiang-Huai areas during 4–7 July 1991. *Plateau Meteorlogy*, **14**, 270–280. (in Chinese)

Derber, J. C., 1987: Variational four-dimensional analysis using quasi-geostrophic constraints. *Mon. Wea. Rev.*, **115**, 998–1008.

Gao Jidong, and Chou Jifan, 1994: Two kinds of inverse problems in NWP and a numerical method–Ideal field experiment. *Acta Meteorologica Sinica,* **52**(2), 129–137. (in Chinese)

LeDimet, F., and O. Talagrand, 1986: Variational algorithms for analysis and assimilation of meteorological observations: Theoretical aspects. *Tellus*, **38A**, 97–110.

Lewis, J. M., and J. C. Derber, 1985: The use of adjoint equation to solve a variational adjustment problem with advective constraints. *Tellus*, **37A**, 309–322.

Navon, I. M., and D. M. Legler, 1987: Conjugate-gradient methods for large-scale minimization in meteorology. *Mon. Wea. Rev.*, **115**, 1479–1502.

Navon, I. M., X. Zou, J. Derber, and J. Sela, 1992: Variational data assimilation with an adiabatic version of the NMC spectral model. *Mon. Wea. Rev.*, **120**, 1433–1446.

Talagrand, O., and P. Curtier, 1987: Variational assimilation of meteorological observations with the adjoint vorticity equation. Part I: Theory. *Quart. J. Roy. Meteor. Soc.*, **113**, 1311–1328.

Wang Bin, Xiaolei Zou, and Jiang Zhu, 2000a: Data assimilation and its applications. *Proc. Natl. Acad. Sci. U.S.A.*, **97**(21), 11143–11144.

Wang Yunfeng, and Wang Bin, 2003: The variational assimilation experiment of GPS bending angle. *Adv. Atmos. Sci.*, **20**(3), 479–486.

Wang Yunfeng, Wu Rongsheng, Wang Yuan, and Pan Yinong, 2000b: A simple method of calculating the optimal step size in 4DVAR technique. *Adv. Atmos. Sci.*, **17**(3), 433–444.

Zhu Jiang, 1995：Four-dimensional data quality control. *Acta Meteorologica Sinica,* **54**(3), 480–487. (in Chinese)

Zhu Min, Lu Hancheng, and Yu Zhihao, 1998: Study of positive feedback mechanism for meso-α-scale cyclone growing on Meiyu front. *Chinese Journal of Atmospheric Sciences*, **22**(3), 312–320.

Zhou Xiaoping, Zhao Sixiong, and Zhang Baoyan, 1984. A numerical simulation of the meso-low formation on mei-yu front. *Chinese Journal of Atmospheric Sciences*, **8**, 353–361. (in Chinese)

Zou, X., and Q. Xiao, 1999: Studies on the initialization and simulation of a mature hurricane using a variational bogus data assimilation scheme. *J. Atmos. Sci.*, **57**, 836–860.

Zou, X., I. M. Navon, and J. Sela, 1993: Control of gravitational oscillations in variational data assimilation. *Mon. Wea. Rev.*, **121**, 272–289.

Zou, X., B. Wang, H. Liu, R. A. Anthes, T. Matsumura, and Y.-J. Zhu, 2000: Use of GPS/MET refraction angles in three-dimentional variational analysis. *Quart. J. Roy. Meteor. Soc.*, **126**, 3013–3040.